DFT MODELING OF SWCNT GROWTH ON IRON CATALYST

G. L. Gutsev *, M. D. Mochena
Department of Physics, Florida A&M University, Tallahassee, Florida 32307
C. W. Bauschlicher Jr.
Mail Stop 230-3 NASA Ames Research Center, Moffett Field, CA 94035

ABSTRACT

We performed simulations of initial stages of a carbon nanotube growth catalyzed by iron particles using all-electron density functional theory with generalized gradient approximation for the exchange-correlation functional. The systems studied are $Fe_4 + C_n$ for n=7-25, $Fe_{10} + C_{15}$, and $Fe_{10}C_{15} + 10C$. In addition, we performed a detailed study of development of different isomers in the C_n series, n=7-25.

1. INTRODUCTION

Single-walled carbon nanotubes (SWCNT) are expected to have an enormous impact on various technological areas related to fabrication of composite materials, sensors, hydrogen storages, protective coatings, and computer memories. The SWCNTs are produced typically from hydrocarbons [1], alcohol [2], and graphite [3]. The method of catalytic chemical vapor deposition (CCVD) [1] makes use of high temperatures to produce carbon and a supported catalyst to initiate the carbon nanotube growth. The catalyst needs restoration after each cycle. Carbon nanotubes grown using this method are often multi-walled, while single-walled nanotubes are of more interest from a technological point of view. On the contrary, the high-pressure high-temperature HiPco [4] method is continuous and its floating or gas-phase catalyst is formed *in situ* from iron pentacarbonyl $Fe(CO)_5$. Using carbon monoxide as feedstock is rather intriguing, because CO is one of the most stable diatomics with the measured bond strength of 11.09 eV. Carbon nanotubes produced in this process are always single-walled and are believed to nucleate and grow via the Boudouard disproportionation reaction $CO + CO \rightarrow C_{SWCNT} + CO_2$. However, the mechanism of carbon nanotube growth is not well understood.

In order to gain insight into carbon nucleation in the HiPco process, we have performed all-electron density functional theory calculations with a generalized gradient approximation (DFT-GGA) on Fe_nC [5], Fe_nCO (n≤6) [6], and $Fe_4C_n(CO)_m$ (n+m≤3, both C and CO are attached to Fe_4) [7] clusters, and estimated the energies of Boudouard CO disproportionation reactions $Fe_4C_n(CO)_m + CO \rightarrow Fe_4C_{n+1}(CO)_{m-1} + CO_2$. The energies found are relatively small and are in the range from -0.26 eV to +0.74 eV. Next, we explored [8] the thermodynamics of CO attachment to a carbon atom that had already precipitated on an iron cluster due to a preceding Boudouard reaction and evaluated the energetics of CO disproportionation reactions $Fe_4C_n(CO)_m + CO \rightarrow Fe_4C_{n+1}(CO)_{m-1} + CO_2$ for higher coverage (n+m≤5). We choose Fe_4^-, Fe_4, and Fe_4^+ clusters since the Fe_4^+ cluster is known to catalyze the growth of benzene from ethylene and cyclopropane in a low-pressure gas-phase process. The number of iron atoms in the clusters formed in the Hipco process ranges from ~10 to ~300 and it is not clear if smaller iron clusters Fe_3 to Fe_{10} can technologically be effective for the SWCNT growth because of different restrictions such as coalescence of small clusters. However, one can anticipate that our computations using computationally less demanding Fe_4 clusters are capable of reproducing the essentials in initiating the SWCNT growth. According to the results of our previous computations, dimerization of carbon atoms is preferable in Fe_4C_4, Fe_4C_5 and its ions, while C_3 trimers form in the ground states of Fe_4C_6 and its ions. Since attachment of COs followed by subsequent Boudouard reaction leads to precipitation of carbon atoms, we considered next the trends in rearrangement of carbon atoms in the lowest energy isomers of clusters Fe_4C_n, n=7-20 [9]. This work discusses some results from Ref. [9] and presents the results of our simulations using Fe_{10} and Fe_4C_{15} clusters.

2. COMPUTATIONAL DETAILS

The Gaussian 98 and 03 programs [10,11] were used. We have used the 6-311+G* basis set (15s11p6d1f)/[10s7p4d1f] [12] and (12s6p1d)/[5s4p1d] [13] for Fe and C, respectively. In some computations involving Fe_{10} and Fe_4C_{15}, we used a smaller 6-31G basis for carbon atoms. Our previous study [14-16] of bare iron clusters and 3d-metal dimers showed that results obtained using many of the DFT-GGA methods included in Gaussian 98 and 03 programs are rather similar; however, the BPW91 vibrational frequencies appear to be less sensitive to the quality of the grid used in the numerical integration than some of the other functionals. On this ground, we choose the BPW91 method, where the exchange-correlation functional is comprised of the Becke's exchange [17] and Perdew-Wang's correlation [18].

The geometry of each cluster was optimized without imposing any symmetry constraints. Iron clusters possess high spin multiplicities and our optimizations of the clusters interacting with carbon species were performed in the range of spin multiplicities enclosing the

Report Documentation Page

Form Approved
OMB No. 0704-0188

1. REPORT DATE	2. REPORT TYPE	3. DATES COVERED
01 NOV 2006	**N/A**	**-**

4. TITLE AND SUBTITLE	5a. CONTRACT NUMBER
DFT Modeling Of Swcnt Growth On Iron Catalyst	5b. GRANT NUMBER
	5c. PROGRAM ELEMENT NUMBER
6. AUTHOR(S)	5d. PROJECT NUMBER
	5e. TASK NUMBER
	5f. WORK UNIT NUMBER
7. PERFORMING ORGANIZATION NAME(S) AND ADDRESS(ES) **Department of Physics, Florida A&M University, Tallahassee, Florida 32307**	8. PERFORMING ORGANIZATION REPORT NUMBER
9. SPONSORING/MONITORING AGENCY NAME(S) AND ADDRESS(ES)	10. SPONSOR/MONITOR'S ACRONYM(S)
	11. SPONSOR/MONITOR'S REPORT NUMBER(S)

12. DISTRIBUTION/AVAILABILITY STATEMENT
Approved for public release, distribution unlimited

13. SUPPLEMENTARY NOTES
See also ADM002075., The original document contains color images.

14. ABSTRACT

15. SUBJECT TERMS

16. SECURITY CLASSIFICATION OF:			17. LIMITATION OF ABSTRACT	18. NUMBER OF PAGES	19a. NAME OF RESPONSIBLE PERSON
a. REPORT	b. ABSTRACT	c. THIS PAGE			
unclassified	**unclassified**	**unclassified**	**UU**	**5**	

ground-state spin multiplicity of the corresponding bare iron cluster. Each geometry optimization was followed by the calculation of the harmonic vibrational frequencies using analytical second derivatives, in order to confirm that the optimized geometry corresponds to a minimum. We computed atomic spin densities using Mulliken [19] approach.

3. GEOMETRICAL STRUCTURES OF Fe_4C_n

Our optimizations revealed a large number of isomers for each Fe_4C_n with a general trend of the carbon ring formation The rings may contain also iron atoms in Fe_4C_6–Fe_4C_{15}. The electronic states of C_n possessing ring-type geometries in the gas phase have the lowest total energies [20] beginning with C_{10}. We found that the formation of pure carbon rings in the lowest total energy of the Fe_4C_n clusters begins with n=15-16. Figure 1 presents the results of our computations for clusters Fe_4C_8 and Fe_4C_9 and shows free carbon clusters C_8 and C_9 optimized at the same level of theory.

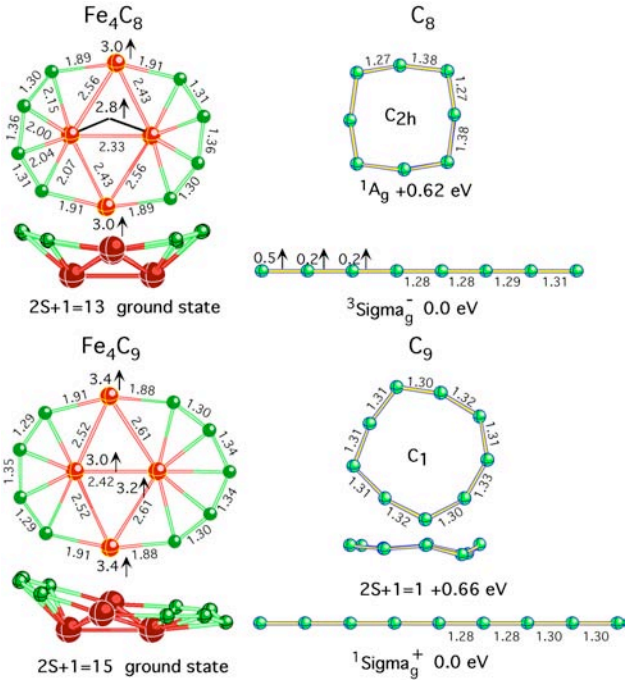

Fig. 1. Top and side views of the ground-state Fe_4 clusters with attached carbon C_8 and C_9 species. The ground and first excited ring states of the latter are shown in the right-hand side. Bond lengths are in Å, excess electronic densities at iron sites are in electrons.

As is seen, carbon atoms form ring structures containing two iron atoms in Fe_4C_8 and in Fe_4C_9, while the ground states of C_8 and C_9 are linear. The ring structures of C_8 and C_9 are above the ground states by about 0.6 eV. The ground-state of the C_8^- and C_9^- anions are also linear. As for the C_n^- anions, there are near-linear states that were a subject of experimental [21] and theoretical [22] studies. According to Ref. [22] and our computations performed with a larger basis set than that used in Ref. [22], the anion ring structure is more stable than a nearly linear one up to n = 14. (Note that optimizations of C_n^- anions imposing $D_{\infty h}$ constraints produce transition states beginning with n=10.) It appears that this number is critical for formation of carbon ring structures on the top of an iron catalyst since there is a charge transfer from iron particles to a more electronegative carbon chain. Figure 2 shows that Fe_4C_{10} contains a ring with two inserted iron atoms while Fe_4C_{14} forms a ring with one inserted iron atom.

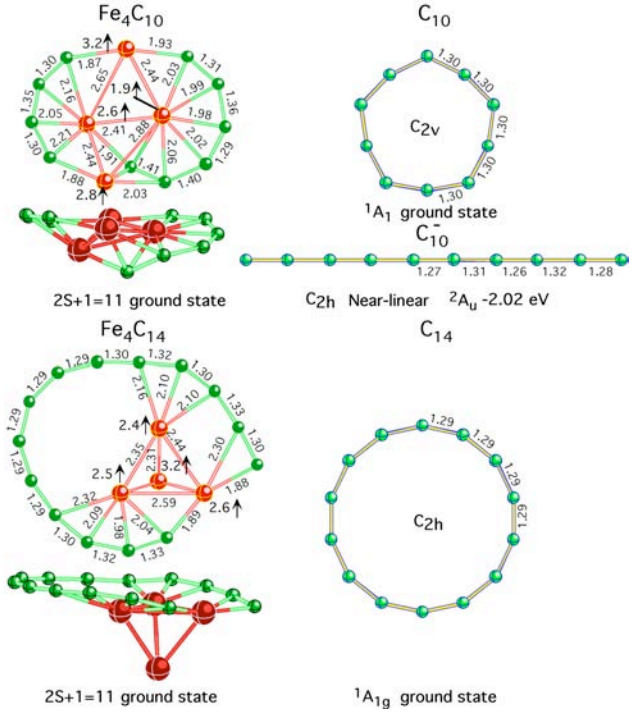

Fig. 2. Top and side views of the ground-state Fe_4C_{10} and Fe_4C_{14} clusters together with the ground states of of C_{10}, C_{10}^-, and C_{14}.

In Fe_4C_{15}, there is a competition between configurations containing a pure C_{15} ring and a C_{15} ring with an iron atom inserted inside the ring. The pure carbon ring structure on the top of Fe_4 becomes favorable in Fe_4 + C_{16}. The lowest energy state of Fe_4 + C_{20} correspond to a C_{19} ring around the cluster and one carbon atom attached to a face of the iron cluster.

In order to gain insight which geometrical structure corresponds to the lowest energy state in C_n we performed optimizations [9] of C_n up to n=25. The first fullerene-type structure with 12 carbon pentagons appears at n=20, but the ring structure is the lowest energy one, followed by a bowl (flake-type) structure, and a fullerene (or cage) structure. Increasing the n number to n=25, we found the ring structures to correspond to the lowest energy states for n = 21, 22, 23, and 25, while the lowest

energy state corresponds to a flake composed of seven hexagons for n=24. At this size, there appears the smallest fullerene possessing two hexagons in addition to 12 pentagons. The results of our optimizations for n=24 are presented in Fig. 4. There are a large number of different shape isomers; some of them are shown in the figure. The triplet states are higher for each flake, ring, or fullerene structures.

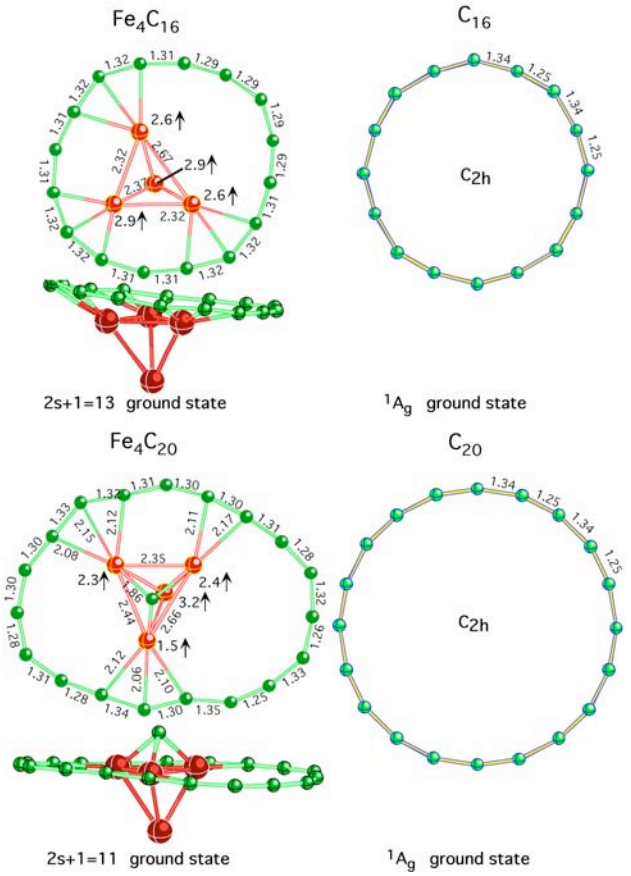

Fig. 3. Top and side views of the ground-state Fe_4 clusters interacting with C_{16} and C_{20}.

4. ISOMERS OF Fe_{10} AND $Fe_{10}C_{15}$

To explore the influence of an iron cluster size, we have optimized several isomers of Fe_{10}. Next, we added a C_{15} ring to one of the isomers in different positions: on the top of long and short sides and wrapped around the center part of the cluster. The results of our optimizations are presented in Fig. 5.

We found that the carbon ring placed along the larger side has acquired one inserted iron atom. This configuration corresponds to the lowest energy state. The ring placed over a shorter side of the iron cluster slightly changes the perfect ring shape and attaches perpendicular to the iron cluster. The C_{15} ring placed around the center shifts during lengthy optimization cycles to the cluster tip while the initial bi-octahedral Fe_{10} configuration transforms to another isomer configuration. The carbon ring placed above the tip is tilted to be nearly parallel to a Fe_3 edge. The latter two $Fe_{10}C_{15}$ isomers are nearly degenerate in total energy and are above the ground state by about 3 eV. The binding energy gain in the ground state apparently comes from breaking a C–C bond and the formation of two Fe–C bonds. This is apparently related with the shape of the surface and does not happen when C_{15} is attached to a shorter side

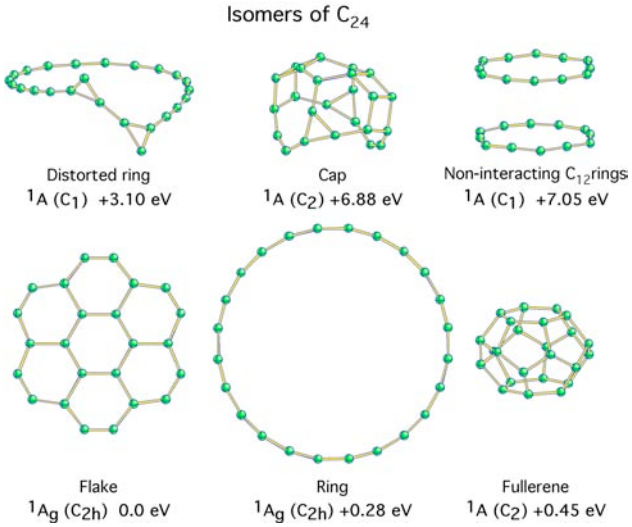

Fig. 4. .Different isomers of C_{24}.

One could speculate that the upward growth on the tilted ring might produce a carbon nanotube with a certain chirality. That is, the part of the cluster surface, which initiates the carbon ring, is related to the chirality of a SWNT grown from the corresponding carbon ring.

5. SIMULATED $Fe_{10}C_{15}$ + 10C GROWTH

In order to gain an insight how carbon atoms attach to a ring formed on an iron particle, we chose a Fe_4C_{15} isomer with a ring C_{15} pattern and added 10 carbon atoms randomly placed at the distance of 5 Å above the ring. Initial and final configurations together with several intermediate configurations obtained at different optimization steps are presented in Fig. 6.

It is found that carbon atoms may form first dimers and trimers in correspondence with experimental observations of such a formation in arc discharges. Next, chains are formed, while the final configuration correspond to a cage with an open 15-carbon ring.

CONCLUSION

Our simulations at a rather reliable DFT-GGA level show that the prime role of a catalyst is to assemble carbon atoms in the optimal gas-phase configuration of C_n that

corresponds to a ring configuration for a rather large n. The surface topology of a catalyst particle is most likely

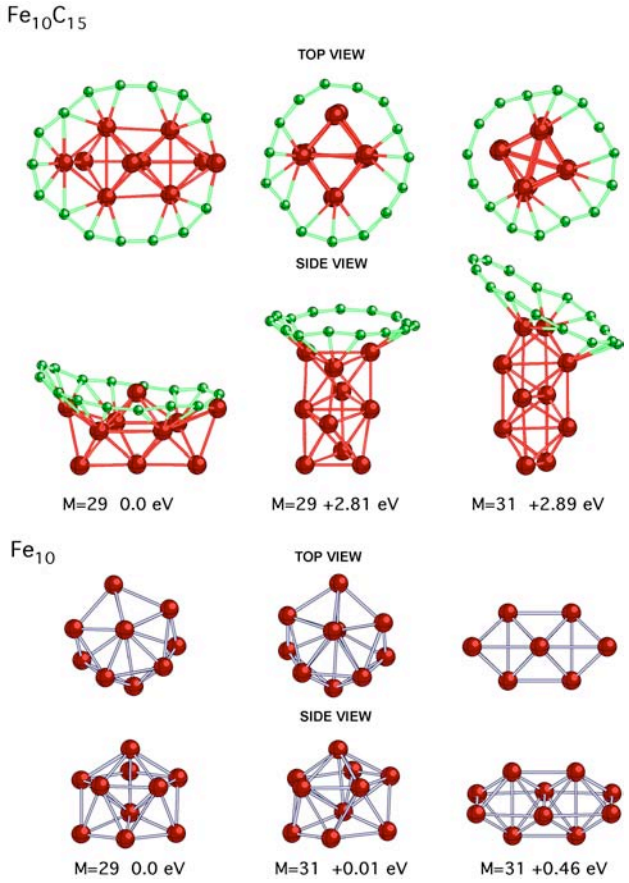

Fig. 5. Different lowest energy isomers of Fe_{10} $Fe_{10}C_{15}$

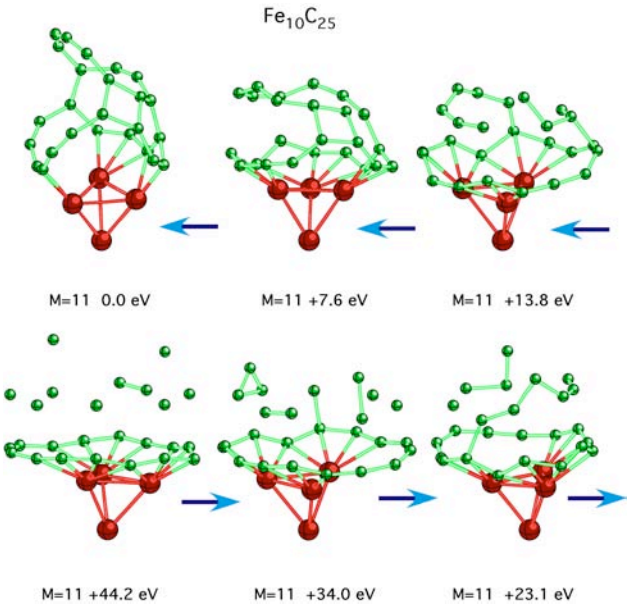

Fig. 6. Configurations obtained in optimizations of $Fe_{10}C_{15}$ + 10C.

responsible for the chirality of a carbon nanotube grown from a seed ring.

ACKNOWLEDGEMENT

This work was supported in part by the Army High Performance Computing Research Center (AHPCRC) under the auspices of the Department of the Army, Army Research Laboratory (ARL) under cooperative Agreement DAAD19-01-2-0014. The content of which does not necessary reflect the position or the policy of the government, and no official endorsement should be inferred.

REFERENCES

1. Su, M., Liu, J.: A scalable CVD method for the synthesis of single-walled carbon nanotubes with high catalyst productivity, *Chem. Phys. Lett.* **322** (2000) 321-326.

2. Maruyama, S., Murakami, Y., Shibuta, Y., Miyauchi, Y., Chiashi, S.: Generation of Single-Walled Carbon Nanotubes from Alcohol and Generation Mechanism by Molecular Dynamics Simulations, *J. Nanosci. Nanotech.* **4** (2004) 360-367.

3. Arepalli, S.: Laser Ablation Process for Single-Walled Carbon Nanotube Production, *J. Nanosci. Nanotech.* **4** (2004) 317-325.

4. Nikolaev, P., Bronikowski, M.J., Bradley, R.K., Rohmund, F., Colbert, D.T., Smith, K.A., Smalley, R.E.: Gas-phase catalytic growth of single-walled carbon nanotubes from carbon monoxide**,** *Chem. Phys. Lett,* **313** (1999) 91-97.

5. Gutsev, G.L., Bauschlicher, C.W., Jr.: Interaction of carbon atoms with Fe_n, Fe_n^-, and Fe_n^+ clusters (n=1–6), *Chem. Phys.* **291** (2003) 27-40.

6. Gutsev, G.L., Bauschlicher, Jr., C.W. : Structure of neutral and charged Fe_nCO clusters (n = 1–6) and energetics of the $Fe_nCO + CO$ $Fe_nC + CO_2$ reaction, *J. Chem. Phys.* **119** (2003) 368-3690.

7. Gutsev, G.L., Mochena, M.D., Bauschlicher, C.W., Jr.: Structure and properties of Fe_4 with different coverage by C and CO, J. Phys. Chem. 108 (2004) 11409-11418.

8. Gutsev, G.L., Mochena, M.D., Bauschlicher, C.W., Jr.: All-electron DFT modeling of SWCNT growth on iron catalysts from carbon monoxide feedstock, *J. Nanosci. Nanotech.*, **6**, (2006) 1281-1289.

9. Gutsev, G.L., Mochena, M.D., Bauschlicher, C.W., Jr.: to be published.

10. *Gaussian 98*, Revision A.11, M. J. Frisch, et. al. Gaussian, Inc., Pittsburgh PA, 1998.

11. G*aussian 03,* Revision B.05*,* D.01*,* Frisch*,* M. J. et. al. Gaussian, Inc., Pittsburgh PA, 2003.

12. Raghavachari, K., Trucks, G. W.: Highly correlated systems. Excitation energies of first row transition metals Sc–Cu, *The Journal of Chemical Physics* **91**, (1989) 1062-1065.

13. Frisch, M. J., Pople, J. A., Binkley, J. S.: Self-consistent molecular orbital methods 25. Supplementary functions for Gaussian basis sets, J. Chem. Phys. **80**, (1984) 3265-3269.

14. Gutsev, G.L.,Bauschlicher, C.W., Jr.: Electron Affinities, Ionization Energies, and Fragmentation Energies of Fen Clusters (n) 2-6): A Density Functional Theory Study, *J. Phys. Chem. A* 107 (2003) 7013-7023.

15. Gutsev, G.L.,Bauschlicher, C.W., Jr.: Chemical Bonding, Electron Affinity, and Ionization Energies of the Homonuclear 3d Metal Dimers, *J. Phys. Chem. A* 107 (2003) 4755-4767.

16 Gutsev, G.L., Mochena, M.D., Jena, P., Bauschlicher, C.W., Jr., Partridge III, H.: Periodic table of 3d-metal dimers and their ions, J. Chem. Phys. 121 (2004) 8785-8796.

17. Becke, A.D.: Density-functional exchange-energy approximation with correct asymptotic behavior, *Phys. Rev. A* 38 (1988) 3098-3100.

18. Perdew, J.P., Wang, Y.: Accurate and simple analytic representation of the electron-gas correlation energy, *Phys. Rev. B* 45 (1992) 13244-13249.

19. Mulliken, R.S.: Electronic Population Analysis on LCAO-MO Molecular Wave Functions. IV. Bonding and Antibonding in LCAO and Valence-Bond Theories, *J. Chem. Phys.* **23** (1955) 2343-2346.

20. Yang, S., Taylor, K.J., Craycraft, M.J., Conceicao, J., Pettiette, C.L., Cheshnovsky, O., Smalley, R.E.: UPS of 2–30-atom carbon clusters: Chains and rings, *Chem. Phys. Lett.* 144 (1988) 431-436.

21. Kohno, M., Suzuki, S., Shiromaru, H., Moriwaki, T., Achiba, Y.: Ultraviolet photoelectron spectroscopy on the linear conformer of negatively charged carbon clusters C_n^- ($10 \le n \le 16$), *Chem. Phys. Lett.* **282** (1998) 330-334.

22. Lépine, F., Allouche, A. R., Baguenard, B., Bordas, Ch., Aubert-Frécon, M.: Computed Electron Affinity of Carbon Clusters C_n up to n = 20 and Fragmentation Energy of Anions, *J. Phys. Chem. A* 106 (2002) 7177-7183.

23. An, W., Gao, Y., Bulusu, S., Zeng, X. C.: Ab initio calculation of bowl, cage, and ring isomers of C_{20} and C_{20}^-, J. Chem. Phys. 122 (2005) 204109-1--204109-8.

24. Moravsky, A.P., Wexler, E.M., Loutfy, R. O.: Growth of carbon nanotubes by arc discharge and laser ablation, Chapter 3 in "*Carbon nanotubes. Science and applications*" (Editor: M. Meyyappan, CRC Press LLC, Boca Raton, 2005).